

# Bidirectional Teleportation using Fisher Information

C. Seida<sup>1</sup>, A. El Allati<sup>2,3</sup>, N. Metwally<sup>4,5</sup>, and Y. Hassouni<sup>1</sup>

<sup>1</sup>ESMAR, Mohammed V University, Faculty of Sciences, Rabat, Morocco

<sup>2</sup>Laboratory of R&D in Engineering Sciences, Faculty of Sciences and Techniques Al-Hoceima, Abdelmalek Essaadi University, Tétouan, Morocco

<sup>3</sup>The Abdus Salam International Center for Theoretical Physics, Strada Costiera 11, Miramare-Trieste, Italy

<sup>4</sup>Math. Dept., College of Science, University of Bahrain, P. O. Box 32038 Kingdom of Bahrain

<sup>5</sup>Math. Dept. Faculty of Science, Aswan University, Aswan, Egypt

July 24, 2020

---

In this contribution, we reformulated the bidirectional teleportation protocol suggested in [7], by means of Bloch vectors as well as the local operations are represented by using Pauli operators. Analytical and numerical calculations for the teleported state and Fisher information are introduced. It is shown that both quantities depend on the initial state settings of the teleported qubits and their triggers. The Fidelities and the Fisher information of the bidirectionally teleported states are maximized when the qubit and its trigger are polarized in the same direction. The minimum values are predicted if both initial qubits have different polarization or non-zero phase. The maximum values of the Fidelity and the quantum Fisher information are the same, but they are predicted at different polarization angles. We display that the multi-parameter form is much better than the single parameter form, where it satisfies the bounds of classical, entangled systems and the uncertainty principle.

---

Keywords: Quantum Fisher information, Estimation, Bidirectional Teleportation.

## 1 Introduction

Quantum teleportation is a process to transmit quantum information between two distant partners, Alice and Bob by using a pre-shared entanglement and classical communication [1]. Over the last twenty years, many modified protocols of quantum teleportation have been proposed, such as the bidirectional quantum teleportation (*BQT*) and the controlled bidirectional quantum teleportation (*CBQT*) protocols. Moreover, these protocols are designed to transfer quantum states simultaneously between the two users. The *CBQT* protocols necessitate an intervention from a third part (Charlie) to accomplish the task. In 2001, *Huelga et al.* [2] discussed the remote implementation of non-local unitary gates using the teleportation in opposite sides, which is bidirectional quantum teleportation. *Zha et al.* [3] proposed a controlled bidirectional teleportation scheme using five qubit cluster state. *Lie et al.* [4] suggested a scheme by using GHZ-Bell composite state. *Zadeh et al.* [5] presented a BQT of two-qubit states by using eight qubits entangled state. *Choudhury et al.* [6] proposed a protocol based on a quantum channel of eleven qubits entangled state to transmit three-qubit *W* state. In the context of non-perfect Teleportation, *Kiktenko et al.* [7] examined a non-perfect protocol of BQT where Alice and Bob transfer a noisy version of their states to each other using a single bell state as a quantum channel.

In some situations, it is not needed to teleport the global information of the state, but only the information of one parameter or multiparameter of the system. The QFI plays a primordial role in the estimation of an unknown parameter through the Cramer-Rao bound [8, 9, 10]. Furthermore, the quantum Fisher information matrix QFIM, provides a tool to determine the precision in any multiparametric estimation protocol. Besides the quantum estimation, the QFI and the QFIM are crucial concepts in Quantum metrology [11, 12], quantum phase transition [13, 14] and entanglement detection [15]. Many efforts have been devoted to investigate the behavior of the QFI in different systems. Metwally *et al.* [16] estimated the teleported and the gained parameters by means of Fisher information in a non-inertial frame. El Anouz *et al.* [17] discussed the unidirectional teleportation of QFI in one and two-qubit

states. Xiao *et al.* [18] studied the QFI teleportation under decoherence by utilizing the partial measurements. Jafarzadeh *et al.* [19] investigated how thermal noise affects the quantum resources and quantum Fisher information (QFI) teleportation.

In the present work, we consider two legitimates users who can transfer their states to each other following *Kiktenko* protocol [7]. We use a single Bell state as a quantum channel to teleport the parameters of the initial states in two opposite directions. The Fidelity of the Bidirectional teleported states between users is discussed, and the estimation of weight parameters of the teleported states Bidirectionally is quantified using QFI. We show that, the QFI and the Fidelity of the bidirectional teleportation depend on the initial states of the teleported qubits as well as on the states of the Triggers. Where, the maximum values of the Fidelity and the quantum Fisher information are the same, but they are predicted at different polarization angles. Also, we display that the multi-parameter estimation is much better than the single parameter form.

The paper is structured as follows. In Sec.2 we briefly review the bidirectional quantum teleportation protocol of *Kiktenko et.al.*[7] where we described it by using Bloch vector and Pauli operators representation. The Fidelities of the bidirectional teleportation states are investigated for different initial state settings in Sec.2.5. The mathematical formals of the quantum Fisher information for a single and multi-parameter are described in Sec.3. Finally, we summarize our results in Sec.4.

## 2 Bidirectional teleportation protocol

In this framework, we use a protocol proposed by *Kiktenko et al.* [7] to transfer information from Bob to Alice as well as from Alice to Bob, i.e., bidirectional teleportation. This protocol is based on a single Bell state, two trigger qubits and classical communication in both directions.

### 2.1 Preparing the initial states

In this section, we review briefly the proposed protocol of *Kiktenko et al.* [7], where the users initially shared an entangled state of Bell type. Let's consider that Alice and Bob share the Bell state :

$$|B_{a,b}\rangle = \frac{1}{\sqrt{2}}(|0_a 0_b\rangle + |1_a 1_b\rangle), \quad (1)$$

where "a" and "b" refer to Alice and Bob respectively. However, since we are interested in estimating the teleported parameters by using quantum Fisher information, we have to describe the procedure of this protocol by means of the Bloch vectors. Therefore, we write the initial Bell state as:

$$\rho_B = \frac{1}{4}(\hat{I} + \hat{\sigma}_x^{(a)} \hat{\tau}_x^{(b)} - \hat{\sigma}_y^{(a)} \hat{\tau}_y^{(b)} + \hat{\sigma}_z^{(a)} \hat{\tau}_z^{(b)}), \quad (2)$$

where  $\hat{\sigma}_i^{(a)}$  and  $\hat{\tau}_i^{(b)}$  (for  $i = x, y, z$ ), represent the Pauli operators of Alice's qubit and Bob's qubit, respectively [20]. Let us assume that Alice and Bob are given two different states,  $|Q_a\rangle$  and  $|Q_b\rangle$  to be bilateral teleported, such as

$$|Q_a\rangle = \cos\left(\frac{\theta_a}{2}\right)|0_a\rangle + e^{i\phi_a} \sin\left(\frac{\theta_a}{2}\right)|1_a\rangle, \quad |Q_b\rangle = \cos\left(\frac{\theta_b}{2}\right)|0_b\rangle + e^{i\phi_b} \sin\left(\frac{\theta_b}{2}\right)|1_b\rangle. \quad (3)$$

Similarly, these qubits can be represented by their Bloch vectors as:

$$\rho_q^{(a)} = \frac{1}{2}\left(\hat{I} + \sum_{i=x,y,z} a_i \hat{\sigma}_i^{(a)}\right), \quad \rho_q^{(b)} = \frac{1}{2}\left(\hat{I} + \sum_{i=x,y,z} b_i \hat{\tau}_i^{(b)}\right), \quad (4)$$

where  $a_i$  and  $b_i$  (for  $i = x, y, z$ ) are the Bloch vectors of Alice's qubit and Bob's qubit, respectively. The aim of the users is exchanging these states between them. Further, each user has two different types of qubits; the trigger qubits which they are defined initially as,

$$|T_a, 0\rangle = \cos\left(\frac{\tilde{\theta}_a}{2}\right)|0_a\rangle + \sin\left(\frac{\tilde{\theta}_a}{2}\right)|1_a\rangle, \quad |T_b, 0\rangle = \cos\left(\frac{\tilde{\theta}_b}{2}\right)|0_b\rangle + \sin\left(\frac{\tilde{\theta}_b}{2}\right)|1_b\rangle, \quad (5)$$

these states become in the Bloch vectors like

$$\rho_{T_a} = \frac{1}{2} \left( \hat{I} + \sum_{i=x,y,z} t_i^{(a)} \hat{\sigma}_i^{(a)} \right), \quad \rho_{T_b} = \frac{1}{2} \left( \hat{I} + \sum_{i=x,y,z} t_i^{(b)} \hat{\tau}_i^{(b)} \right), \quad (6)$$

whereas  $t_i^{(a)}$  ( $t_i^{(b)}$ ) are the Bloch vectors of Alice's (Bob's) Trigger. Additionally, two storage qubits for Alice,  $|S_a^{(1)}\rangle, |S_a^{(2)}\rangle$  and two for Bob,  $|S_b^{(1)}\rangle, |S_b^{(2)}\rangle$ . It is assumed that these qubits are initially prepared in a vacuum state, i.e.,  $|S_j^{(i)}\rangle = |0\rangle, i = 1, 2$  and  $j = a, b$ . These states may be represented by Pauli operators as;  $\rho_{s_a}^{(i)} = \frac{1}{2}(1 + \hat{\sigma}_z^{(a)})$ ,  $i = 1, 2$  and  $\rho_{s_b}^{(i)} = \frac{1}{2}(1 + \hat{\tau}_z^{(b)})$ . These types of qubits are used as a storage of the projective measurement outcomes. All these types of qubits are described clearly in the circuit (Figure:1).

## 2.2 Local Operation

The partners Alice and Bob perform two types of local measurements by the *CNOT* gate and the Toffoli gate (*CCNOT*). These two types of gates are used widely in the context of quantum purification [21]. It is more convenient to perform the *CNOT* operations using Pauli's operators. However, in the computational basis, the *CNOT* operation is defined as shown in Table (1). In addition to the *CNOT* operation, the users need to apply what is called the Toffoli gate. This gate is defined such that the target qubit pairs change only when the two control qubits are in the state  $|1\rangle$ . In a generic form, one can write its effect as *CCNOT* $|abc\rangle = |ab, c \oplus a.b\rangle$ , where the *CCNOT* gate may be defined by using the Pauli operators as,

$$\begin{aligned} CCNOT = \frac{1}{4} & \left[ (1 + \hat{\sigma}_z^{(1)})(1 + \hat{\sigma}_z^{(2)})\hat{\sigma}_x^{(3)} + (1 + \hat{\sigma}_z^{(1)})(1 - \hat{\sigma}_z^{(2)}) \right. \\ & \left. + (1 - \hat{\sigma}_z^{(1)})(1 + \hat{\sigma}_z^{(2)}) + (1 - \hat{\sigma}_z^{(1)})(1 - \hat{\sigma}_z^{(2)}) \right]. \end{aligned} \quad (7)$$

	$\hat{I}^{(2)}$	$\hat{\sigma}_x^{(2)}$	$\hat{\sigma}_y^{(2)}$	$\hat{\sigma}_z^{(2)}$
$\hat{I}^{(1)}$	1	$\hat{\sigma}_x^{(1)}\hat{\sigma}_x^{(2)}$	$\hat{\sigma}_y^{(1)}\hat{\sigma}_x^{(2)}$	$\hat{\sigma}_z^{(1)}$
$\hat{\sigma}_x^{(1)}$	$\hat{\sigma}_x^{(2)}$	$\hat{\sigma}_x^{(1)}$	$\hat{\sigma}_y^{(1)}$	$\hat{\sigma}_z^{(1)}\hat{\sigma}_x^{(2)}$
$\hat{\sigma}_y^{(1)}$	$\hat{\sigma}_z^{(1)}\hat{\sigma}_y^{(2)}$	$\hat{\sigma}_y^{(1)}\hat{\sigma}_z^{(2)}$	$-\hat{\sigma}_x^{(1)}\hat{\sigma}_z^{(2)}$	$\hat{\sigma}_y^{(2)}$
$\hat{\sigma}_z^{(1)}$	$\hat{\sigma}_z^{(1)}\hat{\sigma}_z^{(2)}$	$-\hat{\sigma}_y^{(1)}\hat{\sigma}_y^{(2)}$	$\hat{\sigma}_x^{(1)}\hat{\sigma}_y^{(2)}$	$\hat{\sigma}_z^{(2)}$

Table 1: Bilateral *CNOT* operation between the two qubits which is defined by  $\hat{\sigma}_\mu^{(1)}$  and  $\hat{\sigma}_\mu^{(2)}$ .

## 2.3 Performing the Protocol

In the following, we describe the duty of the users to perform the suggested protocol step by step as shown in Figure 1.

- *From Alice to Bob*

1. *Step one:*

The users prepare their initial state, which consists of 10 qubits, by using the states Eqs.(1-6). This state may be written as:

$$|\psi_s\rangle = |B_a Q_a S_a^{(1)} S_a^{(2)} T_a\rangle |B_b Q_b S_b^{(1)} S_b^{(2)} T_b\rangle. \quad (8)$$

2. *Step two:*

The users apply the *CNOT* gate with  $|Q_{a,b}\rangle$  are control qubits and the Bell qubits  $|B_{a,b}\rangle$  as target qubits as,

$$CNOT|\psi_s\rangle = CNOT|B_a Q_a S_a^{(1)} S_a^{(2)} T_a\rangle CNOT|B_b Q_b S_b^{(1)} S_b^{(2)} T_b\rangle,$$

followed by applying the Hadamard gates on the qubits  $|Q_{a,b}\rangle$  in the previous output results

$$H(CNOT|\psi_s\rangle) = H(CNOT|B_a Q_a S_a^{(1)} S_a^{(2)} T_a\rangle) H(CNOT|B_b Q_b S_b^{(1)} S_b^{(2)} T_b\rangle). \quad (9)$$

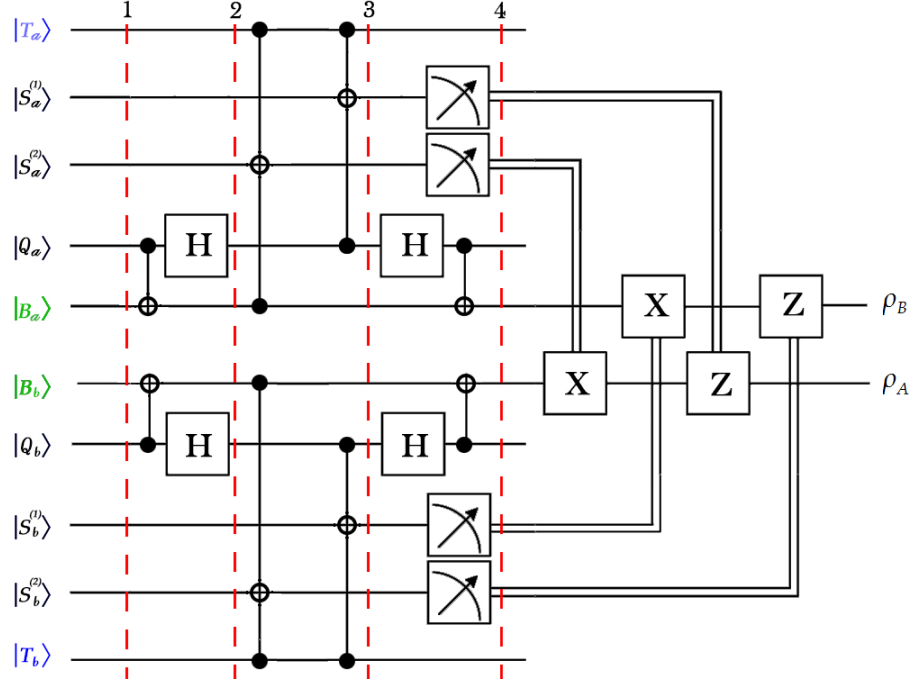


Figure 1: Quantum circuit of the bidirectional teleportation between Alice and Bob using a single Bell state (Eq. (1)), two trigger qubits  $|T_a\rangle$  and  $|T_b\rangle$ . The gates  $X$ ,  $Z$  and  $H$  denote the Pauli and Hadamard gates respectively.  $\bullet$  and  $\oplus$  indicate the control and target qubits of  $CNOT$  and  $Toffoli$  gates respectively. All measurement outcomes (0 or 1) are transmitted via classical channels represented by double lines into gates  $X$  and  $Z$ . The numbers 1, 2, 3 and 4 with dashed red lines stand for the steps of performing the protocol [see Sec. 2.3.]

3. Step three:

Alice and Bob perform two  $CCNOT$  gate. In the first one, the triggers  $|T_{a,b}\rangle$  and the Bell pairs  $|B_{a,b}\rangle$  play the role of the control qubits and  $|S_{a,b}^{(2)}\rangle$  as a target qubit. While in the second  $CCNOT$  the triggers  $|T_{a,b}\rangle$  and  $|Q_{a,b}\rangle$  as a control qubits and  $|S_{a,b}^{(1)}\rangle$  is the target qubit to get:

$$CCNOT\left(H\left(CNOT|\psi_s\rangle\right)\right) = CCNOT\left(H\left(CNOT|B_aQ_aS_a^{(1)}S_a^{(2)}T_a\rangle\right)\right) \otimes CCNOT\left(H\left(CNOT|B_bQ_bS_b^{(1)}S_b^{(2)}T_b\rangle\right)\right) \quad (10)$$

4. Step Four:

The measurement's results are stored in the qubits  $|S_a^{(1)}\rangle$  and  $|S_a^{(2)}\rangle$ . These results are sent by classical channel to Bob. Based on Alice's measurements, Bob performs the adequate local operations  $(\hat{X}, \hat{Y}, \hat{Z}, \hat{I})$ , on his Bell state particle to recover the state  $|Q_a\rangle$ .

• From Bob to Alice:

Bob may perform the same operation that Alice has done to teleport his state  $|Q_b\rangle$  to Alice.

## 2.4 Implementation of the circuit

The final output of the circuit depends on the initial state of the triggers. However, we have the following possibilities:

1. The initial state of both triggers are initially prepared in the states,  $\rho_{T_a} = \frac{1}{2}(1 + \hat{\sigma}_z^{(a)})$  and  $\rho_{T_b} = \frac{1}{2}(1 + \hat{\tau}_z^{(b)})$ . In this case, each partner obtains the completely mixed state, i.e.,  $\rho_q^{(a)} = \rho_q^{(b)} = \rho_0 = \frac{1}{2}(|0\rangle\langle 0| + |1\rangle\langle 1|)$

2. Alice's and Bob's triggers are prepared in the states  $\rho_{T_a} = \frac{1}{2}(1 - \hat{\sigma}_z^{(a)})$  and  $\rho_{T_b} = \frac{1}{2}(1 - \hat{\tau}_z^{(b)})$ . In this case, Alice and Bob perform a perfect projective measurement with probability:

$$p_i = \text{tr}\{\rho_{T_a}\rho_q^{(a)}\} = \text{tr}\{\rho_{T_b}\rho_q^{(b)}\} = \sin^2(\theta_i/2), \quad i = a, b. \quad (11)$$

The users will end up their protocol by two states, one of them at Alice's side.

$$\rho_{tel}^{(a)} = p_b \bar{p}_a \rho_q^{(b)} + (1 - p_b \bar{p}_a) \rho_0, \quad \bar{p}_a = 1 - p_a \quad (12)$$

and the other in Bob's hand

$$\rho_{tel}^{(b)} = p_a \bar{p}_b \rho_q^{(a)} + (1 - p_a \bar{p}_b) \rho_0, \quad \bar{p}_b = 1 - p_b \quad (13)$$

3. If Alice's trigger qubit is prepared in the state  $\rho_{T_a} = \frac{1}{2}(\hat{I} - \hat{\sigma}_z^{(a)})$  and Bob's trigger qubit is prepared in the state  $\rho_{T_b} = \frac{1}{2}(\hat{I} + \hat{\tau}_z^{(b)})$ , then only Alice has the ability to teleport her qubit to Bob. While, Alice get the completely mixed state i.e., the final state at Alice's hand is  $\rho_{tel}^{(a)} = \rho_0$  and at Bob's hand  $\rho_{tel}^{(b)} = \rho_q^{(a)}$ .

## 2.5 Fidelity of teleportation

To quantify the efficiency of the suggested teleportation protocol, we quantify the fidelity  $\mathcal{F}$  of the teleported state. It measures the similarity between the input state  $\rho_q^{(a)}$  ( $\rho_q^{(b)}$ ) and the output state  $\rho_{tel}^{(b)}$  ( $\rho_{tel}^{(a)}$ ) respectively. The expression of the fidelity  $\mathcal{F}$  is defined as [22, 23] :

$$\mathcal{F} = \langle Q^i | \rho_{out} | Q^i \rangle, \quad i = a, b \quad (14)$$

with  $|Q^i\rangle$  and  $\rho_{out}$  are the input and the output states respectively. In general, the input states are unknown. The averaged fidelity over all the input states may be described by

$$\mathcal{F}_{avg} = \frac{1}{4\pi} \int_0^\pi d\theta_i \int_0^{2\pi} \mathcal{F}(\theta_i, \phi_i, p_a, p_b) \sin \theta_i d\phi_i, \quad i = a, b \quad (15)$$

where:

$$\mathcal{F}(\theta_i, \phi_i, p_a, p_b) = |c_i|^2 (A_2 + A_1 |c_t|^2) + A_1 (c_i^* s_i c_t s_t^* + s_i^* c_i s_t c_t^*) + |s_i|^2 (A_1 |s_t|^2 + A_2), \quad (16)$$

with different elements  $c_i = \cos(\frac{\theta_i}{2})$ ,  $s_i = \sin(\frac{\theta_i}{2})e^{i\phi_i}$ ,  $c_t = \cos(\frac{\theta_t}{2})$  and  $s_t = \sin(\frac{\theta_t}{2})e^{i\phi_t}$ . Whereas,  $i$  and  $t$  indicate for the initial and the teleported state respectively. The terms  $A_1$  and  $A_2$  depend on the direction of teleportation. i.e, from Alice to Bob  $A_1 = p_a \bar{p}_b$ ,  $A_2 = \frac{1-p_a \bar{p}_b}{2}$ . While, from Bob to Alice  $A_1 = p_b \bar{p}_a$  and  $A_2 = \frac{1-p_b \bar{p}_a}{2}$ .

The fidelity of teleportation between the two users,  $\mathcal{F}^{A \rightarrow B}$  and  $\mathcal{F}^{B \rightarrow A}$  are given by:

$$\mathcal{F}^{(A \rightarrow B)} = \frac{1}{2}(1 + p_a \bar{p}_b), \quad \mathcal{F}^{(B \rightarrow A)} = \frac{1}{2}(1 + p_b \bar{p}_a), \quad (17)$$

where the probabilities may be written as:

$$\begin{aligned} p_a &= \frac{1}{2} \left( 1 + \cos(\tilde{\theta}_a) \cos(\theta_a) + \sin(\tilde{\theta}_a) \sin(\theta_a) \cos \phi_a + \sin(\tilde{\theta}_a) \sin(\theta_a) \sin \phi_a \right), \\ p_b &= \frac{1}{2} \left( 1 + \cos(\tilde{\theta}_b) \cos(\theta_b) + \sin(\tilde{\theta}_b) \sin(\theta_b) \cos \phi_b + \sin(\tilde{\theta}_b) \sin(\theta_b) \sin \phi_b \right). \end{aligned} \quad (18)$$

Now, by using Eqs.(17) and (18), one can obtain the Fidelity of the teleported state for both directions at an initial state setting.

Fig. (2), shows the behavior of the Fidelity of the teleported state from both directions, namely  $\mathcal{F}^{(A \rightarrow B)}$  and  $\mathcal{F}^{(B \rightarrow A)}$ , where it is assumed that the teleported state is initially prepared in the state  $\rho_q^{(a)} = \frac{1}{2}(\hat{I} + \hat{\sigma}_z^{(a)})$  at Alice side, while Bob's teleported state is given by  $\rho_q^{(b)} = \frac{1}{2}(\hat{I} + \hat{\tau}_z^{(b)})$ , namely the users teleport only classical information,

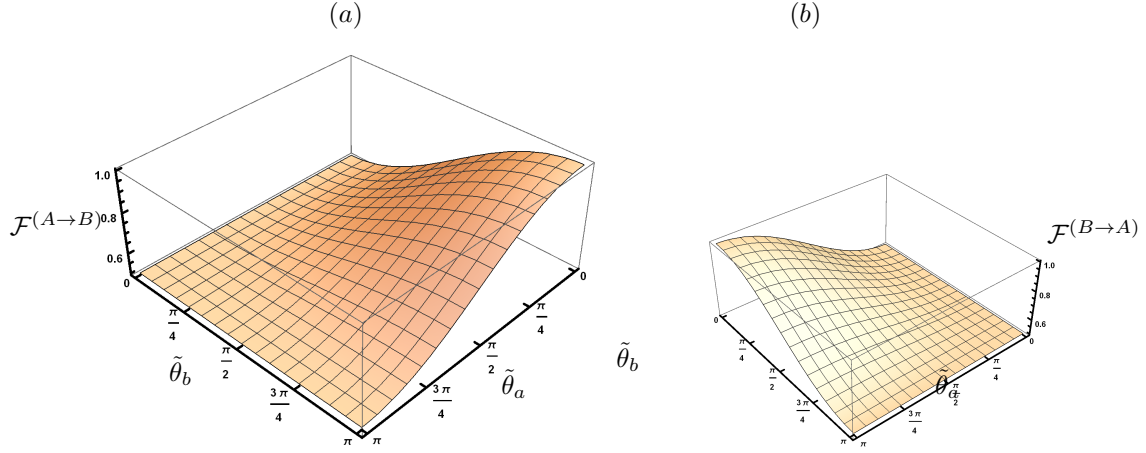


Figure 2: Bidirectional teleportation Fidelity, where the initial states are prepared such that  $\theta_a = \theta_b = 0$  of the initial qubits  $Q_a$  and  $Q_b$ . (a) The fidelity of teleportation  $\mathcal{F}^{(A \rightarrow B)}$  and (b) represents  $\mathcal{F}^{(B \rightarrow A)}$ .

i.e.  $\theta_a = \theta_b = 0$ , while the triggers are prepared in an arbitrary state with  $\phi = 0$ . It is clear that, from Fig.(2a), at any value of  $\tilde{\theta}_b$ , the Fidelity  $\mathcal{F}^{(A \rightarrow B)}$  increases gradually as  $\tilde{\theta}_a$  increases. The maximum Fidelity is reached at  $\tilde{\theta}_a = \pi$ , namely the Alice's trigger is prepared in the state  $\rho_{T_b} = \frac{1}{2}(\hat{I} - \hat{\tau}_z^{(b)})$ . However,  $\mathcal{F}^{(A \rightarrow B)}$ , decreases gradually as  $\tilde{\theta}_b$  increases. The minimum values of  $\mathcal{F}^{(A \rightarrow B)}$  are displayed at  $\tilde{\theta}_a = \pi$ . Fig.(2b), displays the behavior of the fidelity from Bob to Alice,  $\mathcal{F}^{(B \rightarrow A)}$ , where the teleported state is prepared in the state  $\rho_q^{(b)} = \frac{1}{2}(\hat{I} + \hat{\tau}_z^{(b)})$ . The behavior of  $\mathcal{F}^{(A \rightarrow B)}$  is similar to that predicted in Fig.(2a), where the increasing and decreasing of the fidelity depends on the state of Bob's trigger, namely the maximum value is predicted at  $\rho_{T_b} = \frac{1}{2}(\hat{I} - \hat{\tau}_z^{(b)})$ .

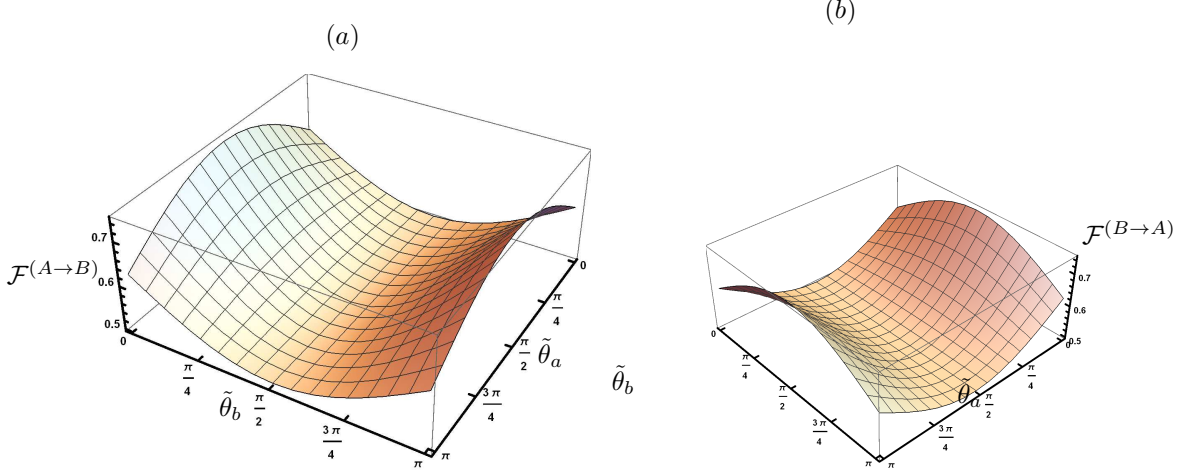


Figure 3: The same as Fig.(2), but the initial teleported state is prepared in the state  $|\psi_q^a\rangle = |\psi_q^b\rangle = \frac{1}{\sqrt{2}}(|0\rangle + |1\rangle)$ , namely  $\theta_a = \theta_b = \pi/2$ .

Teleporting of quantum information via the bidirectional protocol is explored in Fig.(3), where it is assumed that Alice and Bob prepared their states as  $|\psi_q^a\rangle = |\psi_q^b\rangle = \frac{1}{\sqrt{2}}(|0\rangle + |1\rangle)$ , namely we set  $\theta_a = \theta_b = \pi/2$ . It is clear that the maximum values of  $\mathcal{F}^{(A \rightarrow B)}$  and  $\mathcal{F}^{(B \rightarrow A)}$  are smaller than those shown in Fig.(2). The behavior of both Fidelities is similar, where they decrease gradually as the weight of both triggers increases. The minimum values of  $\mathcal{F}^{(A \rightarrow B)}$  and are observed at  $\theta_b = \pi/2$ , while it is increased gradually when Alice's trigger angle  $\tilde{\theta}_a$  increases. The state of both triggers have the same effect on the behavior of  $\mathcal{F}^{(B \rightarrow A)}$ .

In Fig.(4a), we investigate the behavior of  $\mathcal{F}^{(A \rightarrow B)}$ , where we assume that the teleported qubit, Alice and Bob's

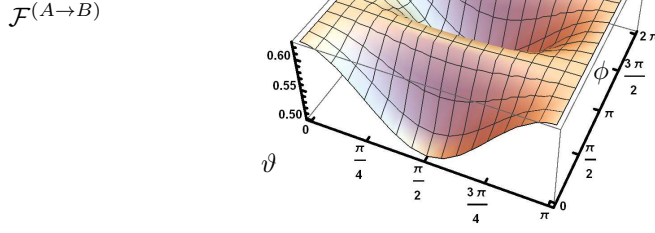


Figure 4: Fidelity of teleportation between Alice and Bob for  $(\phi_a = \phi_b = \phi)$  of the initial qubits  $Qa$  and  $Qb$  and  $\tilde{\theta}_a = \tilde{\theta}_b = \tilde{\theta}_t = \vartheta$ . the Fidelity of teleportation reaches the value of 0.62 as a maximal value.

triggers are prepared on the same state, namely  $\theta_a = \tilde{\theta}_a = \tilde{\theta}_b = \tilde{\theta}_t = \vartheta$ . The behavior of the fidelity shows that, the maximum bound of  $\mathcal{F}^{(A \rightarrow B)}$  is smaller than that displayed in Fig.(2a). The Fidelity decreases gradually as the weight angles of all the qubit decreases. The minimum bounds are predicted at  $\vartheta = \frac{\pi}{2}$ , then increases gradually to reach their maximum values at  $\vartheta = \pi$ . From this figure, it is clear that, the possibility of applying the bidirectional teleportation protocol to teleport classical data is much better than teleporting quantum data. This is predicted at  $\vartheta = \frac{\pi}{2}$ , namely the initial state of the Alice' qubit is prepared in the state,  $|\psi_q^a\rangle = \frac{1}{\sqrt{2}}(|0\rangle + e^{i\phi}|1\rangle)$ . Moreover, as the phase  $\phi$  increases, the Fidelity increase gradually to reach its maximum value at  $\phi \simeq \frac{3\pi}{4}$  at any value of the  $\vartheta$ . In further values of the phase  $\phi$ , the Fidelity decreases gradually to reach its minimum values at  $\phi \simeq \frac{5\pi}{4}$ . This behavior is periodically repeated.

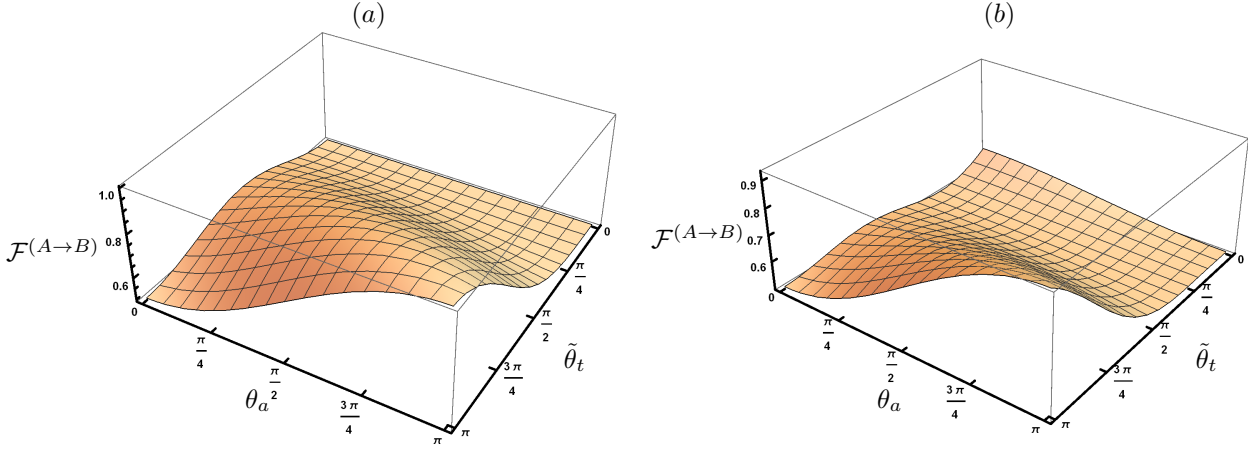


Figure 5: The Fidelity,  $\mathcal{F}^{(A \rightarrow B)}(\theta_a, \tilde{\theta}_t)$ , (a):  $\theta_b = 0$  and (b):  $\theta_b = \pi/4$ .

In the previous investigation, it is assumed that both initial qubits are prepared in the same state. In what follows, we discuss the possibility of bidirectional teleportation, when the partners have different initial states. For this aim, we consider the following figure, where it is assumed that Bob's qubit is initially prepared in the state  $\rho_b = |0\rangle\langle 0|$ , i.e.,  $\theta_b = \pi$ , while Alice's qubit and her triggers are prepared in an arbitrary state with  $\phi_a = \tilde{\phi} = 0$ . Fig.(5a), shows the behavior of the Fidelity  $\mathcal{F}^{(A \rightarrow B)}(\theta_a, \tilde{\theta}_t)$ , where the teleported Bob's qubit is prepared in the state  $\rho_q^{(b)} = \frac{1}{2}(\hat{I} - \hat{\tau}_z^{(b)})$ , i.e  $\theta_b = \frac{\pi}{2}$ . The Fidelity's behavior shows that,  $\mathcal{F}^{(A \rightarrow B)}$  increases as the weight angles of the teleported state and Alice' trigger increase. Therefore, the maximum Fidelity is predicted at  $\theta_a = \tilde{\theta}_t = \pi$ , namely  $\rho_q^{(a)} = \frac{1}{2}(\hat{I} - \hat{\sigma}_z)$ . The effect of the initial state of the trigger shows that at any initial state settings of Alice's qubit, the  $\mathcal{F}^{(A \rightarrow B)}$  increases to reach its maximum bounds. However, at further values of  $\tilde{\theta}_t$ , the Fidelity decreases gradually, where the minimum values are predicted at  $\tilde{\theta}_t = 0$ , i.e., the trigger is prepared in the state  $\rho_{T_a} = \frac{1}{2}(\hat{I} + \hat{\sigma}_z^{(a)})$ . In Fig.(5b), we investigate the effect of different initial state settings of Bob's state, where it is assumed that  $\rho_q^{(b)}$  is prepared at  $\theta_b = \frac{\pi}{4}$ . The behavior is similar to that predicted in Fig.(5a), but the maxi-

imum bounds are smaller than those displayed in Fig.(5a). Moreover, the decay rate is larger compared with that displayed at  $\theta_b = 0$ . In this context, we would like to mention that, the same behavior is predicted for  $\mathcal{F}^{(B \rightarrow A)}(\theta_b, \tilde{\theta}_t)$ .

From Fig(5), one may conclude that the bidirectional Fidelity from Alice to Bob and vice versa, depends on the initial state settings of all the three qubits. However, the maximum Fidelity is attended when all the qubits polarized in the same direction. Moreover, the Fidelity of teleporting classical information is much better than teleporting quantum information.

### 3 Quantum Fisher Information (QFI) and Quantum Fisher information matrix (QFIM)

Many quantum parameters cannot be measured directly, but quantum Fisher information (QFI) may be used to estimate these parameters. Moreover, in the context of quantum teleportation process, it is shown that by teleporting the relevant parameters encoded in the teleported state, one could measure the credibility of the protocol by measuring QFI [17]

#### 3.1 Single parameter estimation

Many quantum parameters cannot be measured directly, but quantum Fisher information(QFI) may be used to estimate these parameters. Moreover, in the context of quantum teleportation process, it is shown that by teleporting the relevant parameters encoded in the teleported state, one could measure the credibility of the protocol by measuring QFI [17].

To calculate the QFI one can use the Bruse distance and the Uhlmann fidelity [24] or using the spectral decomposition of the state  $\rho$ . A simple expression is given in [18] for any single qubit state  $\rho = \frac{1}{2}(1 + \vec{s} \cdot \hat{\sigma})$ . Whereas  $\vec{s} = (s_x, s_y, s_z)$  describes the real Bloch vector and  $\hat{\sigma} = (\hat{\sigma}_x, \hat{\sigma}_y, \hat{\sigma}_z)$  denotes the Pauli matrices.

The amount Fisher information  $\mathcal{F}_\theta$  with respect to the parameter  $\theta$  is written as follows:

$$\mathcal{F}_\theta = \begin{cases} |\partial_\theta \vec{s}|^2 + \frac{(\vec{s} \cdot \partial_\theta \vec{s})^2}{1 - |\vec{s}|^2}, & \text{if } |\vec{s}| < 1 \\ |\partial_\theta \vec{s}|^2, & \text{if } |\vec{s}| = 1, \end{cases} \quad (19)$$

with:  $\partial_\theta = \partial/\partial\theta$ . From Eq. (19) the quantum Fisher information of a pure state ( $|\vec{s}| = 1$ ) is given by the expression  $|\partial_\theta \vec{s}|^2$ . While, for a mixed state ( $|\vec{s}| < 1$ ) is presented by  $|\partial_\theta \vec{s}|^2 + \frac{(\vec{s} \cdot \partial_\theta \vec{s})^2}{1 - |\vec{s}|^2}$ .

According to Ref. [25], the QFI of a single qubit state  $|\psi\rangle$  is defined as:

$$\mathcal{F}_\theta = 4(\langle \partial_\theta \psi | \partial_\theta \psi \rangle - |\langle \partial_\theta \psi | \psi \rangle|^2), \quad (20)$$

the expression of the quantum Fisher information in Eq.(20) can be obtained using only the term of the pure state  $|\psi\rangle$ . The QFI in the two previous equations (19) and (20) provides the estimation precision limit of only one parameter, through the *Cramer – Rao* inequality ( $Var(\hat{\theta}) \geq \mathcal{F}^{-1}$ ) [8]; with  $Var(\hat{\theta})$  is the variance of the parameter and  $\mathcal{F}$  is the quantum Fisher information. where the larger QFI represents the better estimation precision. However, the inverse of the QFI for one unknown parameter provides the lower error limit of the parameter estimation. Our main goal is to reach the smallest value of the variance of the parameter.

Now, let us assume that Alice and Bob have prepared their qubits in the states Eq.(4), while the triggers qubits are defined by Eq.(6). The users use the bidirectional protocol as described in (Sec.2), where the final teleported states between the two users are given by the states (12) and (13). In this context, the final teleported states depend on the initial states of all the used qubits. Therefore, our main aim of this section is to investigate the effect of these parameters on the initial weight angle of the teleported state from Alice to Bob or vice versa. However, by using the definition of the quantum Fisher information for a single qubit, (19) and (20), the Fisher information with respect to the weight angle of Alice and Bob qubits are given by  $\mathcal{F}_{\theta_k} = 1, k = a(b)$ . However, the quantum Fisher information for the phase parameter of both qubits is defined as,  $\mathcal{F}_{\phi_k} = \sin(\theta_k)^2, k = a(b)$ . In Bloch representation form, the final state at Alice's and Bob's hands are described by the following Bloch vectors.

$$a_x^{(tel)} = 2p_a\bar{p}_b \cos \phi_a \cos\left(\frac{\theta_a}{2}\right)\sin\left(\frac{\theta_a}{2}\right) \quad , \quad a_y^{(tel)} = -2p_a\bar{p}_b \sin \phi_a \cos\left(\frac{\theta_a}{2}\right)\sin\left(\frac{\theta_a}{2}\right) \quad , \quad a_z^{(tel)} = p_a\bar{p}_b \cos(\theta_a), \quad (21)$$

Alice received the state  $(b_x^{(tel)}, b_y^{(tel)}, b_z^{(tel)})$  by replacing  $p_a\bar{p}_b \leftrightarrow p_b\bar{p}_a$  and  $\theta_a \leftrightarrow \theta_b$ ,  $\phi_a \leftrightarrow \phi_b$  in Eq. (21):

$$b_x^{(tel)} = 2p_b\bar{p}_a \cos \phi_b \cos\left(\frac{\theta_b}{2}\right)\sin\left(\frac{\theta_b}{2}\right) \quad , \quad b_y^{(tel)} = -2p_b\bar{p}_a \sin \phi_b \cos\left(\frac{\theta_b}{2}\right)\sin\left(\frac{\theta_b}{2}\right) \quad , \quad b_z^{(tel)} = p_b\bar{p}_a \cos(\theta_b), \quad (22)$$

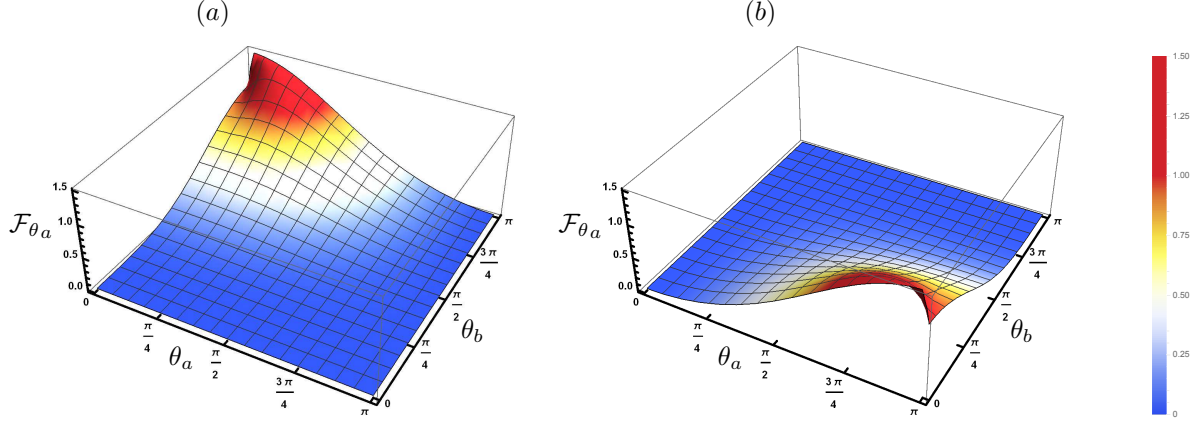


Figure 6: Fisher information of  $\theta_a$ , with arbitrary phase where (a): at  $\tilde{\theta}_a = \tilde{\theta}_b = 0$  and (b): at  $\tilde{\theta}_a = \tilde{\theta}_b = \pi$ .

In Fig.(6), we display the behavior of the teleported Fisher information with respect to the weight parameter  $\theta_a$ ,  $\mathcal{F}_{\theta_a}(\theta_a, \theta_b)$ . Where we consider that the triggers qubits are polarized either on the state  $\rho_T = \frac{1}{2}(\hat{I} + \hat{\sigma}_z)$  or  $\rho_T = \frac{1}{2}(\hat{I} - \hat{\sigma}_z)$ . This figure illustrates that, the maximum bounds of the quantum Fisher information,  $\mathcal{F}_{\theta_a}$  are predicted when both qubit and its trigger have the same polarization direction. As it is displayed from Fig.(6a), the maximum values are predicted at  $\theta_a = 0$ , namely  $\rho_q^{(a)} = \frac{1}{2}(\hat{I} + \hat{\sigma}_z^{(a)})$  and decreases gradually as  $\theta_a$  increases. On the other hand, the initial state settings of Bob state play an important role in the assessment of maximum values of  $\mathcal{F}_\theta$ . However, if Bobs's qubit and Alice' trigger have the same polarization one may estimate the initial weight parameter of  $\theta_a$  with high efficiency. The same behavior is displayed in Fig.(6b), where it is assumed that Alice's and Bob's triggers are prepared in the state  $\rho_T = \frac{1}{2}(\hat{I} - \hat{\tau}_z)$ ,  $t = a, b$ . In this case the  $\mathcal{F}_{\theta_a}$  increases as  $\theta_a$  increases while  $\theta_b$  decreases and the maximum bounds are reached if Alice's qubit and its trigger are prepared in the same state.

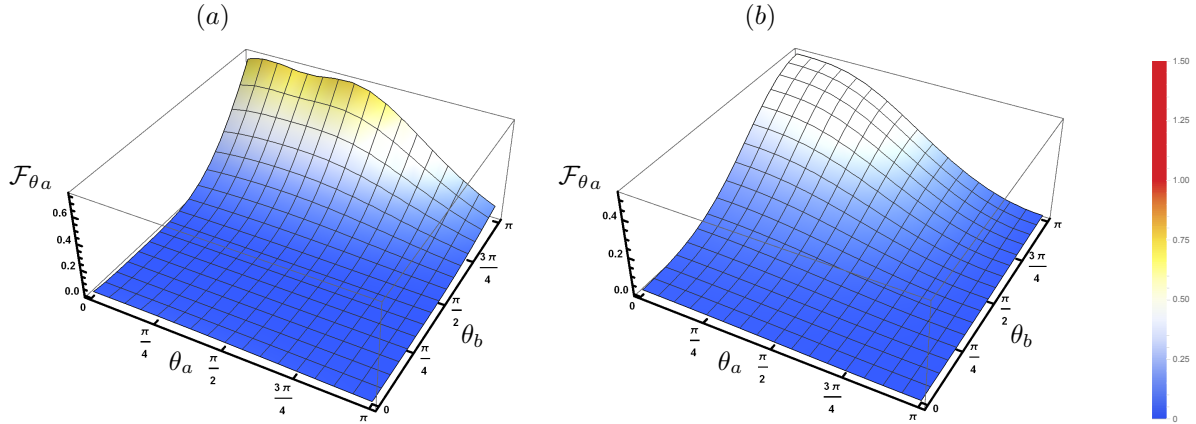


Figure 7: Fisher information  $\mathcal{F}_{\theta_a}$ , with  $\tilde{\theta}_a = \tilde{\theta}_b = \frac{\pi}{4}$  where we set (a):  $\phi = 0$ . (b):  $\phi = \frac{\pi}{2}$

The effect of the phase on the estimation degree of the weight parameter angle  $\theta_a$  is shown in Fig.(7), where two cases are considered of the phase,  $\phi = 0, \frac{\pi}{2}$  in Figs.(7a), (7b), respectively, and it is assumed that the triggers are

prepared by setting  $\tilde{\theta}_a = \tilde{\theta}_b = \frac{\pi}{4}$ . In general, the behavior of  $\mathcal{F}_{\theta_a}$  is similar to that displayed in Fig.(6a). However, the maximum values that are predicted in Fig.(7) are much smaller than those displayed in Fig.(6a). Also, from this figure one may explore that when the initial states of the triggers and the qubits are different, the possibility of estimating the weight parameter decreases. On the other hand, as,  $\theta_b$  increases,  $\mathcal{F}_{\theta}$  increases, but the increasing rate is larger than that displayed in Fig.(6a), where  $\mathcal{F}_{\theta}$  increases gradually. Fig.(7a), displays the effect of larger values of the phase, where we set  $\phi = \frac{\pi}{2}$ . The behavior of the quantum Fisher information is similar to that displayed in Fig.(7a), but the upper bounds are smaller. Moreover, the increasing rate (as  $\theta_b$  increases) and the decreasing rate (as  $\theta_a$  increases) are smoothly compared with those shown in Fig.(7a).

From Fig.(6) and (7), one may conclude that the possibility of maximizing the estimation degree, depends on the initial state of the triggers. The larger bounds are predicted when the qubits and their triggers are polarized in the same direction. The phase parameter plays the control parameter on the whole process, where the maximization of the quantum Fisher information is predicted at  $\phi = 0, \pi$  and  $2\pi$ . Otherwise it is minimized. The minimum values are affected by the initial state preparation of Alice and Bob.

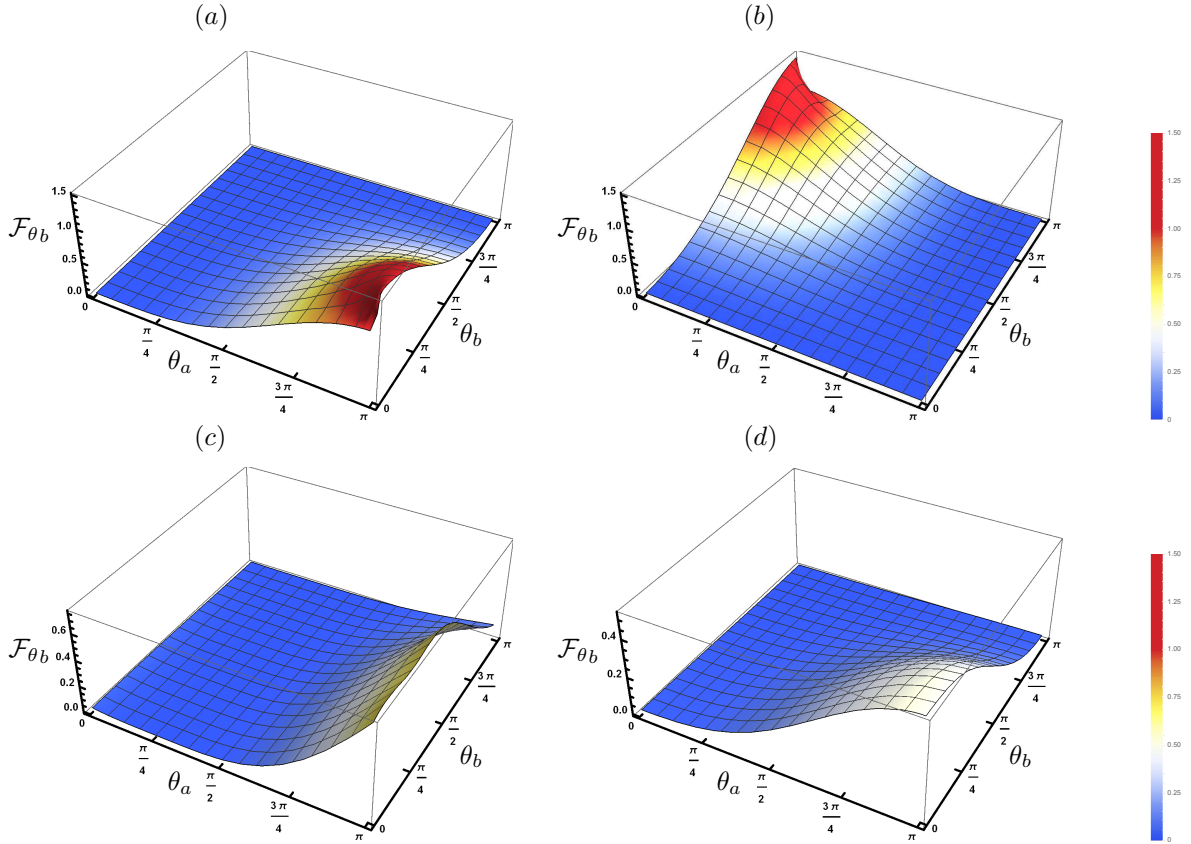


Figure 8: Fisher information  $\mathcal{F}_{\theta_b}$ , where (a) and (b) are the same as Fig. (6), while (c) and (d) are the same as Fig.(7).

In Fig.(8), we summarize the effect of the initial state settings of Alice and Bob's qubit. As well as, the state of their triggers on the behavior of  $\mathcal{F}_b$ . In Fig.(8a), we used to assume that the initial states of the trigger are prepared in the states  $\frac{1}{2}(\hat{I} + \hat{\sigma}_z^{(a)})$  for Alice's trigger, while Bob's trigger is prepared in the state  $\frac{1}{2}(\hat{I} + \hat{\tau}_z^{(b)})$ , where the phase of all the qubits is arbitrary. The behavior is similar to that displayed in Fig.(6), but as the  $\mathcal{F}_{\theta_a}$  increases,  $\mathcal{F}_{\theta_b}$  decreases. This means that, as the information at Alice's hand starts to increase, the information at Bob's hand decreases. Therefore the maximum bounds are predicted at different initial state settings. However, the states of the triggers play the same role as it is played in Fig.(6). As it is shown in Fig.(8b), the maximum bound of  $\mathcal{F}_{\theta_b}$  is shown at  $\theta_b = \pi$ , namely  $\rho_q^{(b)} = \frac{1}{2}(\hat{I} - \hat{\tau}_z^{(b)})$ . This means that the Bob state is prepared on its trigger's state, where  $\rho_T^{(b)} = \frac{1}{2}(\hat{I} - \hat{\tau}_z^{(b)})$ . On the other hand, the minimum values of the quantum Fisher information  $\mathcal{F}_{\theta_b}$  are predicted at  $\theta_b = 0$ , namely  $\rho_q^{(b)} = \frac{1}{2}(\hat{I} + \tau_z^{(b)})$  and  $\rho_q^{(a)} = \frac{1}{2}(\hat{I} - \hat{\sigma}_z^{(b)})$ .

Figs.(8c) and (8d) describe the effect of the phase on the estimation degree of  $\mathcal{F}_{\theta_b}$ , where we assume that the trigger states are prepared with a weight angle  $\tilde{\theta}_a = \tilde{\theta}_b = \frac{\pi}{4}$ . It is clear that the behavior of the quantum Fisher information is similar to that shown of  $\mathcal{F}_{\theta_a}$  as displayed in Fig.(7). However, the maximum bound of  $\mathcal{F}_{\theta_b}$  is displayed at  $\theta_b = \frac{\pi}{4}$ , namely when the weight angle  $\theta_b = \tilde{\theta}_b = \frac{\pi}{4}$ . Moreover at  $\phi_a = \phi_b = \phi = 0$ , the losses on Fisher information due to the difference between the initial state preparation of both qubits. In fact, an additional loss of the quantum Fisher information due to the existence of the phase, where at  $\phi = \frac{\pi}{2}$ , the maximum bounds of  $\mathcal{F}_{\theta_b}$  are smaller than those shown at  $\phi = 0$ .

### 3.2 Multiparameter estimation

The quantum Fisher information matrix (QFIM) provides a tool to determine the precision in the multiparameter estimation. Where the lower bound of the estimation is given by the Cramer Rao inequality [8] as:

$$Cov(\hat{\theta}) \geq \mathcal{F}M^{-1}, \quad (23)$$

with  $\hat{\theta} = \theta_1, \theta_2, \dots$  is a set of parameters can be encoded in the density matrix  $\rho = \rho(\hat{\theta})$  and  $Cov(\hat{\theta})$  is the covariance of the parameters  $\hat{\theta}$ ,  $\mathcal{F}M^{-1}$  is the quantum Fisher information matrix.

The inverse of the QFIM gives the lower error limit of the estimation. The expression of the QFIM [8] is defined as:

$$\mathcal{F}M_{ij} = Tr[\rho \frac{L_i L_j + L_j L_i}{2}] = Tr[\partial_i \rho L_i] = Tr[\partial_j \rho L_j], \quad (24)$$

with  $L_i$  is the symmetric logarithmic derivative corresponds to the parameter  $\theta_i$  which is determined by the equation:

$$\partial_i \rho = \frac{1}{2}(L_i \rho + \rho L_i), \quad (25)$$

using the Eqs. (24) and (25), two expressions of the QFIM can be derived. The first is based on the calculation of the exponential of  $\rho$  and an integral as:

$$\mathcal{F}M_{ij} = Tr[\partial_i \rho L_i] = 2 \int_0^\infty Tr[dte^{-\rho t} \partial_i \rho e^{-\rho t} \partial_i \rho]. \quad (26)$$

The second expression to calculate the QFIM is based on the decomposition of  $\rho$  into eigenvalues  $p_n$  and eigenvectors  $|\psi_n\rangle$  as:

$$\rho = \sum_n p_n |\psi_n\rangle \langle \psi_n| \quad (27)$$

$$\mathcal{F}M_{ij} = 2 \sum_{p_n + p_m > 0} \langle \psi_m | \partial_i \rho | \psi_n \rangle \langle \psi_n | \partial_j \rho | \psi_m \rangle / p_n + p_m \quad (28)$$

A simple expression to calculate the QFIM is given in [26]. For an invertible density matrix  $\hat{\rho}$ , the QFIM can be computed analytically as :

$$\mathcal{F}M_{ij} = 2Vec^\dagger[\partial_i \hat{\rho}] (\hat{\rho}^T \otimes \hat{I} + \hat{I} \otimes \hat{\rho})^{-1} Vec[\partial_j \hat{\rho}], \quad (29)$$

where  $\partial_i = \partial/\partial\theta_i$ ,  $\hat{I}$  is the identity matrix and  $\rho^T$  is the transpose of  $\rho$ .  $Vec[\partial_i \hat{\rho}]$  is the Vector column of the matrix  $\partial_i \hat{\rho}$ . In an explicit form, one can write the matrix representation of the quantum Fisher information matrix with respect to the two parameters  $\theta_a$  and  $\theta_b$  as,

$$\mathcal{F}_{\theta_a, \theta_b} = \begin{pmatrix} \mathcal{F}_{\theta_a, \theta_a} & \mathcal{F}_{\theta_b, \theta_a} \\ \mathcal{F}_{\theta_a, \theta_b} & \mathcal{F}_{\theta_b, \theta_b} \end{pmatrix}, \quad (30)$$

where,

$$\mathcal{F}_{\theta_i, \theta_j} = \begin{cases} (\partial_{\theta_i} \vec{a})(\partial_{\theta_j} \vec{a}) + \frac{(\vec{a} \cdot \partial_{\theta_i} \vec{a})(\vec{a} \cdot \partial_{\theta_j} \vec{a})}{1 - |\vec{a}|^2}, & \text{if } |\vec{a}| < 1 \\ (\partial_{\theta_i} \vec{a})(\partial_{\theta_j} \vec{a}), & \text{if } |\vec{a}| = 1. \end{cases} \quad (31)$$

Explicitly on Alice side the QFIM is given by,

$$\mathcal{F}_{\theta_a, \theta_b}^{Alice} = \frac{1}{1 - (p_b \bar{p}_a)^2} \begin{pmatrix} (p_b \partial_{\theta_a} \bar{p}_a)^2 & p_b \bar{p}_a \partial_{\theta_b} p_b \partial_{\theta_a} \bar{p}_a \\ p_b \bar{p}_a \partial_{\theta_b} p_b \partial_{\theta_a} \bar{p}_a & (p_b \bar{p}_a)^2 (1 - (p_b \bar{p}_a)^2) + (\bar{p}_a \partial_{\theta_b} p_b)^2 \end{pmatrix}. \quad (32)$$

A similar expression is obtained for QFIM at Bob's side, just we switched between the suffix  $a$  and  $b$ . However, the amount of Fisher information at the users Alice (Bob) that injected on the parameters  $\theta_b(\theta_a)$  respectively is given by,

$$\mathcal{F}_{\theta_b} = \frac{(p_b \bar{p}_a)^2 (1 - (p_b \bar{p}_a)^2) + (\bar{p}_a \partial_{\theta_b} p_b)^2}{1 - (p_b \bar{p}_a)^2}, \quad \mathcal{F}_{\theta_a} = \frac{(p_a \bar{p}_b)^2 (1 - (p_a \bar{p}_b)^2) + (\bar{p}_b \partial_{\theta_a} p_a)^2}{1 - (p_a \bar{p}_b)^2}. \quad (33)$$

By using the Cramer-Rao bound for one parameter estimation, one can estimate the single parameter by means of the variance as,

$$\text{Var}(\theta_a)^{Ind} \geq \frac{1 - (p_a \bar{p}_b)^2}{(p_a \bar{p}_b)^2 (1 - (p_a \bar{p}_b)^2) + (\bar{p}_a \partial_{\theta_a} p_a)^2} \quad ; \quad \text{Var}(\theta_b)^{Ind} \geq \frac{1 - (p_b \bar{p}_a)^2}{(p_b \bar{p}_a)^2 (1 - (p_b \bar{p}_a)^2) + (\bar{p}_b \partial_{\theta_b} p_b)^2}, \quad (34)$$

where it is assumed that the estimation process of each parameter is independent. However, the variance estimation of the two parameters  $\theta_a$  and  $\theta_b$  is given simultaneously as [27],

$$\text{Var}(\theta_b)^{Sim} \geq \frac{(p_b \partial_{\theta_b} \bar{p}_a)^2}{\bar{p}_a^2 p_b^4 (\partial_{\theta_a} \bar{p}_a)^2} \quad ; \quad \text{Var}(\theta_a)^{Sim} \geq \frac{(p_a \partial_{\theta_a} \bar{p}_b)^2}{\bar{p}_b^2 p_a^4 (\partial_{\theta_b} \bar{p}_b)^2}. \quad (35)$$

The minimum variance of the two parameters may be described by,

$$\Delta = \frac{V_I(\theta_a)}{V_S(\theta_a)}, \quad \delta = \frac{V_I(\theta_b)}{V_S(\theta_b)}. \quad (36)$$

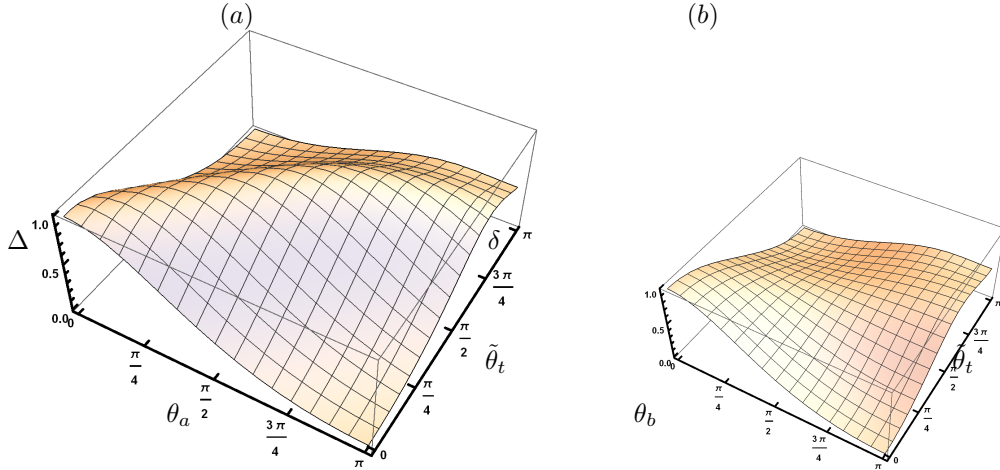


Figure 9: Ratios of estimations  $\Delta$  (for Alice) with  $\theta_b = \frac{\pi}{4}$  and  $\delta$  (for Bob), with  $\theta_a = \frac{\pi}{4}$ , where we set  $\tilde{\theta}_a = \tilde{\theta}_b = \tilde{\theta}_t$ , where we set  $\phi = 0$  for (a,c) and  $\phi = \frac{\pi}{2}$  for (b,d)

In Fig.(9) we investigate the behavior of the ratio variances  $\Delta$  and  $\delta$  for different initial state settings. It is clear that the ratios  $\Delta < 1$ , and  $\delta < 1$  namely  $V_S(\theta_i) > V_I(\theta_i)$ ,  $i = a, b$  and consequently those ratios satisfy, the maximum/minimum probability of quantum mechanics, where  $\Delta$  and  $\delta \in [0, 1]$ . So, the ratios demonstrate the full classical/quantum systems at 0 and 1, respectively. Moreover, these ratios obey the uncertainty principle for  $0 \leq \Delta(\delta) \leq 1$ . On the other hand, for individual estimation, we can see that the quantum Fisher information  $(\mathcal{F}_{\theta_a}(\mathcal{F}_{\theta_b})) > 1$ , which outside the range of entangled systems. Therefore, using the multi-parameter form is much better than the single parameter form. Fig.(9a), describes the behavior of  $\Delta(\theta_a, \theta_t)$  at a particular initial state of Bob's qubit, where we set  $\theta_b = \frac{\pi}{4}$ , with zero-phase for all the qubits. Also, the maximum/minimum bounds are depicted when the qubits and its trigger have the same polarization. As an example, the maximization is predicted at  $\theta_a = \theta_t = 0$  or  $\pi$ , while the minimum values are predicted when  $\theta_a$  and  $\theta_t$  are different. The same behavior is predicted for the ratio  $\delta$ , but the maximum and minimum are displayed at different angles.

## 4 Conclusion

In this contribution, we are interested in bidirectional quantum Fisher information between two users, Alice and Bob. Since the form of the Fisher information is based on Bloch vectors, therefore we reformulated the bidirectional

protocol of Kiktenko in terms of Bloch vectors. It is assumed that, the users' qubits and their trigger's qubits are described by using the Bloch vectors. Moreover, the local operations of CNOT and CCNOT gates are represented by Pauli-operators and the circuit which describes this protocol is introduced clearly.

We have discussed the fidelity of the bidirectional teleported states between the two users, where analytical forms of the fidelity are obtained. These fidelities depend on the initial states of the teleported qubit as well as on the states of the triggers. It is shown that, the fidelity of the teleported state is maximized when the teleported qubit and its trigger are polarized in the same direction. However, the initial state settings of the qubits play an important role in maximizing/minimizing the fidelity of the teleported state, where the maximization is achieved if both qubits are initially prepared in the same direction. The minimization takes place at non-zero phase angle or different initial state settings. The fidelity of the teleported classical information bidirectionally over the quantum channel is much better than teleporting quantum information.

The possibility of estimating the weight parameters of the teleported states bidirectionally is quantified by using quantum Fisher information. An analytical form based on the Bloch vectors is introduced. Similarly, the fidelity depends on the initial states of all the qubits. It is shown that the possibility of maximizing the estimation degree depends on the initial state of the triggers. The larger bounds are predicted when the qubits and their triggers are polarized in the same direction. The phase parameter plays the control parameter on the whole process, where the maximization of the quantum Fisher information is predicted at  $\phi = 0, \pi, 2\pi$ , otherwise it is minimum. The minimum values are affected by the initial state settings of Alice and Bob.

In addition to estimating a single parameter, we quantify the weight parameters of the bidirectional states by means of the variances' ratios. It is shown that the multi-parameter estimation technique is much better than the single parameter estimation, where the ratios running between "0" for fully classical systems and "1" for completely entangled system as well as the uncertainty principle is obeyed. It is shown that, the maxim/minimum estimation of these parameters depends on the initial states of the triggers. Also, as the maximum estimation is predicted at Alice 's side, the minimum estimation is displayed at Bob's side.

Since, the initial states of Alice and Bob, as well as the states of their trigger are similar, therefore the maximum/minimum values of the fidelity of the teleported states and the quantum Fisher information are the same for both directions. However, as soon as Alice got the maximum information, Bob lost all the information and vice versa. Therefore, the maximum bounds of the fidelity and the quantum Fisher information are obtained at different weight angles.

## References

- [1] C.H. Bennett, G. Brassard, C. Crepeau, R. Jozsa, A. Peres, W.K. Wootters, Teleporting an unknown quantum state via dual classical and EinsteinPodolskyRosen channels. *Phys. Rev. Lett.* **70**, 1895 (1993).
- [2] S.F. Huelga, M. Plenio, Quantum remote control: Teleportation of unitary operations. *Phys. Rev. A* **63**, (2001).
- [3] X.W. Zha, Z.C. Zou, J. X. Qi, Bidirectional Quantum Controlled Teleportation via Five-Qubit Cluster State. *International Journal of Theoretical Physics* **52**(6), 1740-1744 (2013).
- [4] Y. Li, L. Nie. Bidirectional Controlled Teleportation by Using a Five-Qubit Composite GHZ-Bell State. *Int J Theor Phys* **52**, 1630 (2013).
- [5] S. Zadeh, M. Sadegh, M. Houshmand, H. Aghababa, Bidirectional teleportation of a two-qubit state by using eight-qubit entangled state as a quantum channel. *International Journal of Theoretical Physics* **56** (7), 2101-2112 (2017).
- [6] B. S. Choudhury, S. Samanta, Bidirectional Teleportation of Three-Qubit Generalized W-States Using Multi-partite Quantum Entanglement. *Physics of Particles and Nuclei Letters* **16** (6), 206-215 (2019).
- [7] E.O.Kiktenko, A. A. Popov, A. K. Fedorov, Bidirectional imperfect quantum teleportation with a single Bell state. *Phys Rev A* **93**(6), 062305 (2016).
- [8] M. G. Paris Paris, Quantum estimation for quantum technology. *Int Journal of Quantum Information* **7**(supp01), 125-137 (2009).

- [9] C. W. Helstrom, Quantum detection and estimation theory. *Journal of Statistical Physics* **1**(2), 231-252 (1969).
- [10] A. S. Holevo, Probabilistic and statistical aspects of quantum theory (Vol. **1**). Springer Science Business Media (2011).
- [11] V. Giovannetti, S. Lloyd, L. Maccone, Quantum metrology. *Phys. Rev. Lett.* **96**, 010401 (2006).
- [12] V. Giovannetti, S. Lloyd, L. Maccone, Advances in quantum metrology. *Nat. Photon.* **5**, 222 (2011).
- [13] T. L. Wang, L. N. Wu, W. Yang, G. R. Jin, N. Lambert, F. Nori, Quantum Fisher information as a signature of the superradiant quantum phase transition. *New Journal of Physics* **16**(6), 063039 (2014).
- [14] U. Marzolino, T. Prosen, Fisher information approach to nonequilibrium phase transitions in a quantum XXZ spin chain with boundary noise, *Physical Review B* **96**(10), 104402 (2017).
- [15] N. Li, S. Luo, Entanglement detection via quantum Fisher information, *Physical Review A* **88**(1), 014301 (2013).
- [16] N. Metwally, Estimation of teleported and gained parameters in a non-inertial frame. *Laser Phys. Lett.* **14**, 045202 (2017).
- [17] K. El Anouz, A. El Allati, N. Metwally, T. Mourabit, Estimating the teleported initial parameters of a single and two-qubit systems. *Applied Physics B* **125**, 11 (2019); N. Metwally, Fisher information of accelerated two-qubit systems, *International Journal of Modern Physics B* Vol. 32, No. **5**, 1850050 (2018).
- [18] X. Xiao, Y. Yao, W. J. Zhong, Y. Li, Y. Xie, Enhancing teleportation of quantum Fisher information by partial measurements. *Phys Rev A* **93** (1), 012307 (2016).
- [19] M. Jafarzadeh, H. R. Jahromi, M. Amniat-Talab, Teleportation of quantum resources and quantum Fisher information under Unruh effect. *Quantum Information Processing* **17**, 165 (2018).
- [20] N. Metwally and A. A. Al Amin, Maximum entangled states and quantum Teleportation via Single Cooper pair Box. *Physica E* **41**, 718-722 (2009); N. Metwally, Teleportation of Accelerated Information. *J. Opt. Soc. Am. B*, Vol. 30, No. **1**, 233-237 (2013).
- [21] N. Metwally, A. S. Obada, More efficient purifying scheme via controlled-controlled Not gate. *Phys Lett A* **352**(1-2), 45-48 (2006).
- [22] K. Wang, R. Yu, X.T. , Z. C. Zhang, Quantum Handshake Beacon in Communication System Using Bidirectional Quantum Teleportation. *International Journal of Theoretical Physics* **58**(1), 121-135 (2019).
- [23] A. El Allati, N. Metwally and Y. Hassouni, Transfer information remotely via noise entangled coherent channels. *Opt. Commun.* **284**, 519526 (2011).
- [24] J. Liu, H. N.Xiong, F. Song, X.Wang, Fidelity susceptibility and quantum Fisher information for density operators with arbitrary ranks. *Physica A: Statistical Mechanics and its Applications* **410**, 167-173(2014).
- [25] J. Liu, H. Yuan, X. M. Lu, X. Wang, Quantum Fisher information matrix and multiparameter estimation. arXiv preprint arXiv:**1907**, 08037 (2019).
- [26] D. afrneq, Simple expression for the quantum Fisher information matrix. *Physical Review A* **97** (4), 042322 (2018).
- [27] Y.Chen, H. Yuan, Maximal quantum Fisher information matrix. *New Journal of Physics* **19** (6), 063023 (2017).

